

# Error Performance Bounds for Tracking a Manoeuvring Target

A. Bessell<sup>a</sup>, B. Ristic<sup>a</sup>, A. Farina<sup>b</sup>, X. Wang<sup>c</sup>, M. S. Arulampalam<sup>a</sup>

<sup>a</sup> DSTO, PO Box 1500, Edinburgh SA 5111, Australia  
{amanda.bessell,branko.ristic,sanjeev.arulampalam}@dsto.defence.gov.au

<sup>b</sup> Alenia Marconi Systems, Via Tiburtina, Rm 12,400, 00131 Rome, Italy  
afarina@amsjv.it

<sup>c</sup> CSSIP, Dept. EEE, University of Melbourne, Parkville Vic.3010, Australia  
xu.wang@ee.mu.oz.au

## Abstract –

*The paper explores the subject of Cramér-Rao type lower bounds for tracking a manoeuvring target. Target dynamics are modelled by the switching of multiple (possibly nonlinear) motion regimes. Two types of bounds are considered. The first is evaluated as the expected value over the regime sequences. The computational complexity of this bound grows exponentially with time. The second bound is applicable only to the deterministic trajectories, and assumes that the knowledge of the particular regime sequence is known. Numerical examples are provided in support of theoretical considerations.*

**Keywords:** Target tracking, Cramer-Rao bound, hybrid estimation, manoeuvring target

## 1 Introduction

In target tracking applications, target dynamics are often modelled by multiple motion regimes (or modes) that cover all possible system behaviour patterns (e.g. manoeuvring and non-manoevring motions) [1]. Formulated in this way, target tracking is a hybrid state estimation problem, characterised by a continuous-valued target state and a discrete-valued regime variable [2]. The target state vector at discrete-time  $k$ ,  $\mathbf{x}_k \in \mathbb{R}^n$ , evolves according to one of possibly multiple nonlinear dynamic models, derived from a stochastic difference (or differential) equation. The discrete regime variable  $r_k$ , is governed by a discrete stochastic

process and takes one of a finite number  $s$  of behaviour modes. The regime switching is usually modelled by a finite state homogeneous Markov chain, with a priori known transition probabilities. The measurement model describes a possibly nonlinear stochastic relationship between the sensor measurement and the target state.

The optimal recursive state estimator in the Bayesian sense requires the complete posterior density of the state to be determined as a function of time. For the described hybrid estimation problem, no closed form optimal analytic solution exists, even when the target motion can be modelled with a *single dynamic model*, i.e.  $s = 1$  [3]. Consequently, various practical solutions to the hybrid estimation problem have been proposed based on approximations [1, Ch.11], [4, Ch.10]. In the absence of a closed-form solution, it would be important to quantify the performance degradation of practical solutions and thus measure the effect of introduced approximations. For nonlinear filtering with a single regime ( $s = 1$ ), the development of a theoretical Cramér-Rao lower bound (CRLB) has received considerable attention [5], [6], [7], [8], [9]. Such a performance bound is very important in practice: it enables us to predict the best achievable performance based on fundamental properties of dynamic and measurement models; it can be used to optimise sensor placement or scheduling; it provides an assessment of the effects of approximations introduced by suboptimal algorithms, etc.

In this paper we explore the theoretical CRLB for the case when  $s \geq 1$ . Two approaches are considered. The derivation of the first is in spirit very similar

to the one presented in [8], and the theoretical solution requires enumeration of an exponentially growing number of regime variable sequences. The second approach assumes that the target trajectory is deterministic, consisting of a few segments of different dynamic motions. This case is often considered in the tracking literature [10, p.280], [1, Sec.11.7.4], [11].

## 2 Problem formulation

Consider the discrete-time nonlinear filtering problem with multiple switching dynamic models and additive Gaussian noise. The target motion is then modelled as follows:

$$\mathbf{x}_k = \mathbf{f}_{k-1}(\mathbf{x}_{k-1}, r_k) + \mathbf{w}_{k-1}(r_k) \quad (1)$$

where  $r_k$  is a regime variable in effect during the time interval from  $k-1$  to  $k$ . The evolution of the regime variable is modelled by a time-homogeneous  $s$ -state first-order Markov chain with transition probabilities:

$$\pi_{ij} \triangleq \Pr\{r_{k+1} = j | r_k = i\} \quad (2)$$

for any  $i, j \in S$  where  $S \triangleq \{1, 2, \dots, s\}$ . The transitional probability matrix (TPM)  $\mathbf{\Pi} = [\pi_{ij}]$  is an  $s \times s$  matrix with elements satisfying  $\pi_{ij} \geq 0$  and  $\sum_{j=1}^s \pi_{ij} = 1$  for each  $i \in S$ . Denote the initial regime probabilities as  $\mu_i \triangleq \Pr\{r_1 = i\}$ , for  $i \in S$ , such that  $\mu_i \geq 0, \forall i \in S$  and  $\sum_{i=1}^s \mu_i = 1$ . Both  $\mathbf{\Pi}$  and  $\mu_i$ 's are assumed known. In addition, the initial target state  $\mathbf{x}_0$  has a known probability density function  $p(\mathbf{x}_0)$ . The remaining terms in (1) are:  $\mathbf{f}_{k-1}(\mathbf{x}_{k-1}, r_k)$  is a nonlinear function which models the evolution of the target state while in regime  $r_k$ ;  $\mathbf{w}_{k-1}(r_k)$  is a zero-mean white Gaussian process noise with nonsingular covariance matrix  $\mathbf{Q}_{k-1}(r_k)$ .

The measurement equation is given by:

$$\mathbf{z}_k = \mathbf{h}_k(\mathbf{x}_k, r_k) + \mathbf{v}_k \quad (3)$$

where  $\mathbf{z}_k \in \mathbb{R}^m$  is the measurement at time  $k$  and  $\mathbf{v}_k$  is zero-mean white Gaussian measurement noise, independent of  $\mathbf{w}_k$ , with nonsingular covariance matrix  $\mathbf{R}_k$ .

Let us define the collection of all measurements up to time  $k$  by  $\mathbf{Z}_k \triangleq \{\mathbf{z}_1, \dots, \mathbf{z}_k\}$ . The aim of a tracking algorithm is to estimate  $p(\mathbf{x}_k, r_k | \mathbf{Z}_k)$ , from which one can derive the state estimate  $\hat{\mathbf{x}}_{k|k}$  and also the estimates of mode probabilities. The objective of this study is the computation of the theoretical CRLB for an unbiased state estimator  $\hat{\mathbf{x}}_{k|k}$ .

## 3 Enumeration method

### 3.1 Derivation

A sequence of regime variables at time  $k$  is a  $k$ -tuple which takes one of  $s^k$  possible realisations of the Markov chain. Let us define a particular sequence as

$$R_k^\ell \triangleq (r_1^\ell, r_2^\ell, \dots, r_k^\ell) \quad (4)$$

where  $l = 1, 2, \dots, s^k$ . The probability that sequence  $R_k^\ell$  will occur can be expressed using the known  $\mathbf{\Pi}$  and  $\mu_i$ 's as follows:

$$P(R_k^\ell) = \left[ \prod_{j=1}^s \mu_j^{\delta(r_1^\ell, j)} \right] \prod_{i=1}^s \left[ \prod_{j=1}^s \pi_{ij}^{n_{ij}(R_k^\ell)} \right] \quad (5)$$

where  $\delta(r_i, j) = 1$  if  $r_i = j$  and zero otherwise and

$$n_{ij}(R_k^\ell) = \sum_{\eta=2}^k \delta(r_{\eta-1}^\ell, i) \delta(r_\eta^\ell, j) \quad (6)$$

is the number of transitions from regime  $i$  to regime  $j$  in the regime sequence  $R_k^\ell$ . For example, if  $s = 2$  and  $k = 9$ , the probability of regime sequence  $\{1, 1, 1, 2, 2, 2, 2, 1, 2\}$  equals  $\mu_1 \pi_{11}^2 \pi_{12}^2 \pi_{21} \pi_{22}^3$ .

Given a particular regime sequence  $R_k^\ell$ , the covariance matrix of an unbiased estimator  $\hat{\mathbf{x}}_{k|k}$  has a lower bound as follows:

$$\mathbb{E} \left\{ (\hat{\mathbf{x}}_{k|k} - \mathbf{x}_k) (\hat{\mathbf{x}}_{k|k} - \mathbf{x}_k)^T \middle| R_k^\ell \right\} \geq [\mathbf{J}_k^\ell]^{-1}, \quad (7)$$

where  $\mathbf{J}_k^\ell$  is the information matrix conditioned on  $R_k^\ell$ . According to [7],  $\mathbf{J}_k^\ell$  can be expressed as:

$$\mathbf{J}_k^\ell = \mathbf{D}_{k-1}^{\ell, 22} - \left[ \mathbf{D}_{k-1}^{\ell, 12} \right]^T \left( \mathbf{J}_{k-1}^\ell + \mathbf{D}_{k-1}^{\ell, 11} \right)^{-1} \mathbf{D}_{k-1}^{\ell, 12} \quad (8)$$

where

$$\mathbf{D}_{k-1}^{\ell, 11} = \mathbb{E} \left\{ [\mathbf{F}_{k-1}^\ell]^T [\mathbf{Q}_{k-1}^\ell]^{-1} \mathbf{F}_{k-1}^\ell \right\} \quad (9)$$

$$\mathbf{D}_{k-1}^{\ell, 12} = -\mathbb{E} \left\{ [\mathbf{F}_{k-1}^\ell]^T \right\} [\mathbf{Q}_{k-1}^\ell]^{-1} \quad (10)$$

$$\mathbf{D}_k^{\ell, 22} = [\mathbf{Q}_{k-1}^\ell]^{-1} + \mathbb{E} \left\{ [\mathbf{H}_k^\ell]^T \mathbf{R}_k^{-1} \mathbf{H}_k^\ell \right\}. \quad (11)$$

with  $\mathbf{Q}_{k-1}^\ell \triangleq \mathbf{Q}_{k-1}(r_k^\ell)$  and Jacobians

$$\mathbf{F}_{k-1}^\ell = \left[ \nabla_{\mathbf{x}_{k-1}} \mathbf{f}_{k-1}^T(\mathbf{x}_{k-1}, r_k^\ell) \right]^T \quad (12)$$

$$\mathbf{H}_k^\ell = \left[ \nabla_{\mathbf{x}_k} \mathbf{h}_k^T(\mathbf{x}_k, r_k^\ell) \right]^T, \quad (13)$$

evaluated at the true state vector. In summary, the computation of the conditional information matrix  $\mathbf{J}_k^\ell$  can be done recursively, using the given regime sequence. Assuming that the initial pdf of the target

state is Gaussian with covariance  $P_0$ , the recursion in (8) begins with

$$\mathbf{J}_0^\ell = \mathbf{P}_0^{-1}. \quad (l = 1, 2, \dots, s^k) \quad (14)$$

The corresponding conditional CRLB is then defined as

$$\text{CRLB}^\ell(\mathbf{x}_k) \triangleq [\mathbf{J}_k^\ell]^{-1}. \quad (15)$$

The unconditional Posterior CRLB for the hybrid estimation problem is defined as the expected value of the conditional CRLBs, i.e.

$$\text{CRLB}(\mathbf{x}_k) = \mathbb{E} \left\{ \text{CRLB}^\ell(\mathbf{x}_k) \right\} \quad (16)$$

where the expectation is taken over the regime sequences. It follows then

$$\text{CRLB}(\mathbf{x}_k) = \sum_{\ell=1}^{s^k} P(R_k^\ell) \cdot [\mathbf{J}_k^\ell]^{-1} \quad (17)$$

where  $P(R_k^\ell)$  is given by (5) and  $\mathbf{J}_k^\ell$  by (8).

### 3.2 Implementation

The implementation of recursion (8) may require a change in the dimension of the information matrix whenever there is a model switch. This is due to the different state vector sizes for different dynamic models (e.g. the constant velocity versus the constant acceleration model). The augmentation or reduction of the information matrix must be done in the inverse matrix domain. For example, suppose an  $n \times n$  information matrix corresponding to model  $i$ ,  $\mathbf{J}_k^\ell(i)$ , has to be augmented to a  $(n+1) \times (n+1)$  matrix corresponding to model  $j$ ,  $\mathbf{J}_k^\ell(j)$ , where  $i, j \in \{1, 2, \dots, s\}$ . Let the additional component (due to augmentation) in the state vector of model  $j$  be the  $(n+1)$ -th component. Then

$$[\mathbf{J}_k^\ell(j)]^{-1} = \begin{bmatrix} [\mathbf{J}_k^\ell(i)]^{-1} & \mathbf{0} \\ \mathbf{0}^T & \sigma_{n+1}^2 \end{bmatrix} \quad (18)$$

where  $\sigma_{n+1}$  denotes the standard deviation of the additional component in model  $j$  and  $\mathbf{0}$  is the  $n$  dimensional zero vector.

The CRLB for nonlinear filtering with switching models given by equation (17), in theory can be computed exactly. In practice, however, the number of possible regime sequences grows exponentially with time and the CRLB can be computed only for small values of  $k$ . In doing so, one can exploit the structure of the transitional probability matrix to limit the number of considered regime sequences in the weighted sum of (17), and thus simplify the computation. The diagonal elements of a typical TPM are much greater than the

non-diagonal elements. This means that the regime sequences with a large number of switches (transitions) are very unlikely and hence can be ignored in the computation of the weighted sum (17). For example, suppose  $s = 2$  and let the TPM be symmetric with elements  $\pi_{11} = \pi_{22} = p$  and  $\pi_{12} = \pi_{21} = (1-p)$ . The probability of having  $\tau$  transitions in a regime sequence of length  $k$  is  $\binom{k-1}{\tau} p^{k-1-\tau} \cdot (1-p)^\tau$ . The number of transitions in a regime sequence of length  $k$  can be regarded as a random variable  $\tau$  with a cumulative distribution:

$$F_k(\tau) = \sum_{i=0}^{\tau} \binom{k-1}{i} p^{k-1-i} (1-p)^i. \quad (19)$$

This function is plotted in Figure 1 for  $k = 20$  and  $p = 0.95, 0.90$  and  $0.85$ . Note from Figure 1 that for (say)  $p = 0.90$ , all regime sequences with more than  $\tau = 5$  transitions can be safely ignored in the calculation of (17), because their probabilities are negligible.

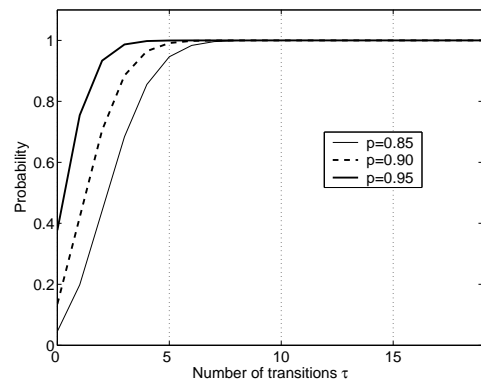


Figure 1: Cumulative distribution of  $\tau$  for  $k = 20$

### 3.3 Numerical examples

Consider a target moving in two dimensions with  $s = 2$  dynamic models and no process noise.

**Model 1.** The constant velocity (CV) model, with state vector defined as  $\mathbf{x}_k = [x_k \dot{x}_k y_k \dot{y}_k]^T$  and function  $\mathbf{f}_{k-1}(\mathbf{x}_{k-1}, r_k = 1) = \mathbf{F}_{cv} \mathbf{x}_k$ , where  $x$  and  $y$  are the target position in cartesian coordinates,  $\dot{x}$  and  $\dot{y}$  are the target velocities and

$$\mathbf{F}_{cv} = \begin{bmatrix} 1 & T & 0 & 0 \\ 0 & 1 & 0 & 0 \\ 0 & 0 & 1 & T \\ 0 & 0 & 0 & 1 \end{bmatrix}. \quad (20)$$

**Model 2.** The constant acceleration (CA) model, with  $\mathbf{x}_k = [x_k \dot{x}_k \ddot{x}_k y_k \dot{y}_k \ddot{y}_k]^T$  and

$\mathbf{f}_{k-1}(\mathbf{x}_{k-1}, r_k = 2) = \mathbf{F}_{ca}\mathbf{x}_k$ , where  $\ddot{x}$  and  $\ddot{y}$  are the target acceleration components in cartesian coordinates and

$$\mathbf{F}_{ca} = \begin{bmatrix} 1 & T & \frac{T^2}{2} & 0 & 0 & 0 \\ 0 & 1 & T & 0 & 0 & 0 \\ 0 & 0 & 1 & 0 & 0 & 0 \\ 0 & 0 & 0 & 1 & T & \frac{T^2}{2} \\ 0 & 0 & 0 & 0 & 1 & T \\ 0 & 0 & 0 & 0 & 0 & 1 \end{bmatrix}. \quad (21)$$

The sampling interval is  $T = 3\text{s}$ . The TPM is symmetric with  $p = 0.90$  and initial model probabilities are  $\mu_1 = 1$  and  $\mu_2 = 0$ .

The measurements  $\mathbf{z}_k$  of equation (3) consist of target position with  $\mathbf{h}_k(\mathbf{x}_k, r_k = 1) = \mathbf{H}_{cv}\mathbf{x}_k$  and  $\mathbf{h}_k(\mathbf{x}_k, r_k = 2) = \mathbf{H}_{ca}\mathbf{x}_k$  where

$$\mathbf{H}_{cv} = \begin{bmatrix} 1 & 0 & 0 & 0 \\ 0 & 0 & 1 & 0 \end{bmatrix} \quad \mathbf{H}_{ca} = \begin{bmatrix} 1 & 0 & 0 & 0 & 0 & 0 \\ 0 & 0 & 0 & 1 & 0 & 0 \end{bmatrix} \quad (22)$$

and

$$\mathbf{R} = \begin{bmatrix} \sigma_x^2 & 0 \\ 0 & \sigma_y^2 \end{bmatrix} \quad (23)$$

where  $\sigma_x = \sigma_y = 200\text{m}$ .

The  $\mathbf{P}_0$  matrix introduced in equation (14) is specified for the CV case only (since  $\mu_2 = 0$ ) as:

$$\mathbf{P}_0 = \begin{bmatrix} \sigma_x^2 & 0 & 0 & 0 \\ 0 & \sigma_{\dot{x}}^2 & 0 & 0 \\ 0 & 0 & \sigma_y^2 & 0 \\ 0 & 0 & 0 & \sigma_{\dot{y}}^2 \end{bmatrix} \quad (24)$$

where  $\sigma_{\dot{x}} = \sigma_{\dot{y}} = 150\text{m/s}$ .

When there is a switch from the CV model to the CA model, the information matrix is augmented as described by (18). The additional components in this case are the acceleration in the  $x$  and  $y$  directions. The standard deviations we use in this augmentation are  $\sigma_{\ddot{x}} = \sigma_{\ddot{y}} = 1.5g$ , where  $g = 9.81\text{ m/s}^2$ .

Next we compute the CRLB via (17) for the described experimental setup. Figure 2 shows the square root of the CRLB for the estimated target position  $p_k = \sqrt{x_k^2 + y_k^2}$ . This CRLB is defined as:

$$CRLB(p_k) = CRLB(x_k) + CRLB(y_k) \quad (25)$$

There is a total of 15 scans and we plot  $\sqrt{CRLB(p_k)}$  at different levels of approximation, with up to 2, 4 and 6 transitions in regime sequences  $R_k^\ell$ . Observe from Figure 2 that the difference in  $\sqrt{CRLB(p_k)}$  with up to 4 and up to 6 transitions is very small. This confirms our earlier conjecture that the regime sequences with a large number of transitions can be ignored in the computation of the CRLB, when the diagonal elements of the TPM are dominant.

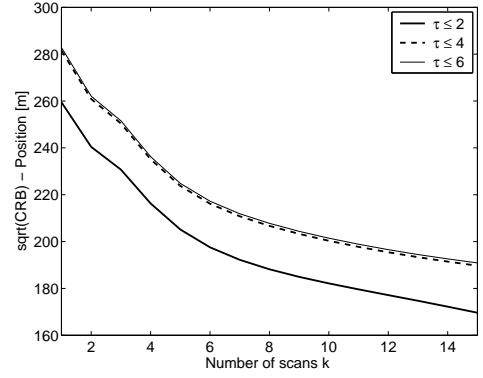


Figure 2: The  $\sqrt{CRLB(p_k)}$  computed using regime sequences with up to 2, 4 and 6 transitions.

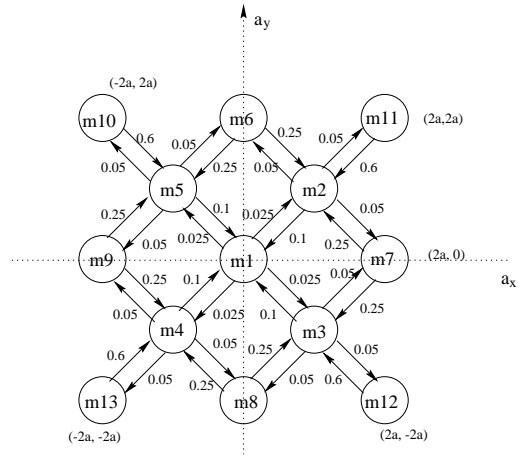


Figure 3: Digraph of maneuver model set of 13 models.

In order to confirm the CRLB shown in Figure 2, we performed Monte Carlo simulations and estimated the RMS error of a Variable Structure (VS-IMM) filter. The performance of a VS-IMM is essentially the same as an IMM, but can provide considerable maneuver capability coverage for the unknown maneuver model, without significant computational cost [12]. The maneuver model set in the VS-IMM is represented by a finite collection of quantized acceleration vectors, over a continuous acceleration space. Figure 3 shows the digraph of a maneuver model set used in our simulation, where  $a = 10\text{m/s}^2$ . The VS-IMM filter is based on the minimal sub-model set switching algorithm described in detail in [12].

In simulations, the initial target state vector is  $\mathbf{x}_0 = [10000\text{m}, -220\text{m/s}, 0\text{m/s}^2, 20000\text{m}, 0\text{m/s}, 0\text{m/s}^2]^T$ . The generated target trajectory is purely random due to the Markovian switching, and over time may end

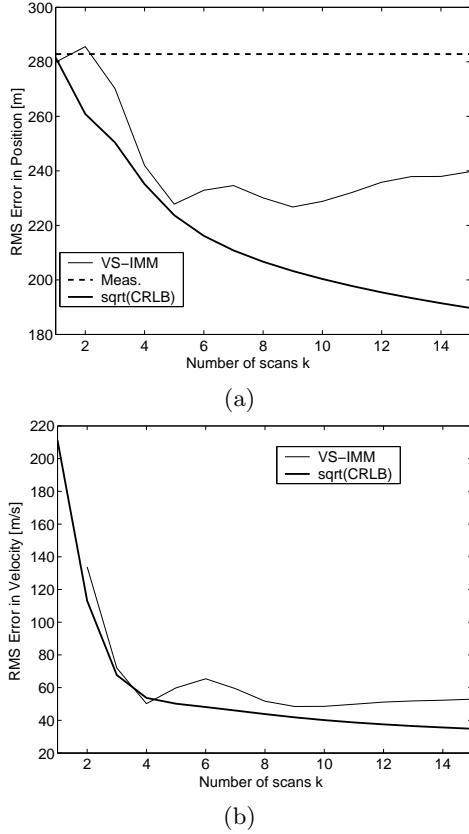


Figure 4: RMS error in (a) position and (b) velocity vs the  $\sqrt{\text{CRLB}}$

up anywhere, depending on the particular regime sequence. When the target is in the CA regime, the acceleration in  $x$  and  $y$  are  $-1g$  and  $+1g$ , respectively.

The results of 10000 Monte Carlo runs are shown in Figure 4. The dashed line in Figure 4.(a) indicates the measurement accuracy - this is the upper bound of performance. The theoretical error bound  $\sqrt{\text{CRLB}}$  is the lower bound. The RMS error in position of the VS-IMM appears to be between the two bounds. The RMS error in velocity is in much better agreement with the  $\sqrt{\text{CRLB}}$  curve.

## 4 Deterministic trajectory

### 4.1 Background

In practice, the error performance of algorithms for tracking manoeuvring targets is often evaluated using a deterministic trajectory. The tracking books [10, p.280], [1, Sec.11.7.4] as well as the widely publicised benchmark tracking problem [11] also consider deterministic trajectories. Typically, the trajectory consists of a few fixed-length segments of interleaved non-manoeuving and manoeuvring motion. For this kind

of problem, one can compute a type of CRLB which assumes that the correct regime sequence  $R_k^*$  is known a priori. By setting the probability  $P(R_k^*)$  to 1 and the probabilities of other regime sequences to zero, it follows from (17) that  $\text{CRLB}(\mathbf{x}_k) = [\mathbf{J}_k^*]^{-1}$ , where  $\mathbf{J}_k^*$  is computed via (8) using the correct regime sequence. However, since the trajectory is assumed to be purely deterministic (no process noise, deterministic regime sequence) equation (8) for computation of  $\mathbf{J}_k^*$ , can be simplified as follows [5]:

$$\mathbf{J}_k^* = \left[ \mathbf{F}_{k-1}^* [\mathbf{J}_{k-1}^*]^{-1} [\mathbf{F}_{k-1}^*]^T \right]^{-1} + [\mathbf{H}_k^*]^T \mathbf{R}^{-1} \mathbf{H}_k^* \quad (26)$$

This bound is conservative (too optimistic) because it assumes the knowledge of the regime sequence, which the filtering algorithm actually needs to estimate. This can be shown as follows. From its definition, the error covariance matrix  $\mathbf{C}_k$  of an unbiased estimator  $\hat{\mathbf{x}}_{k|k}$  is bounded from below as:

$$\mathbf{C}_k = \mathbb{E} \left\{ (\hat{\mathbf{x}}_{k|k} - \mathbf{x}_k) (\hat{\mathbf{x}}_{k|k} - \mathbf{x}_k)^T \right\} \geq \mathbf{J}_k^{-1} \quad (27)$$

where  $\mathbf{J}_k$  is defined as [13]

$$\mathbf{J}_k = \mathbb{E} \left\{ [\nabla_{\mathbf{x}_k} \log p(\mathbf{x}_k, \mathbf{Z}_k)] [\nabla_{\mathbf{x}_k} \log p(\mathbf{x}_k, \mathbf{Z}_k)]^T \right\}. \quad (28)$$

From (7) it follows that:

$$\mathbf{C}_k^* = \mathbb{E} \left\{ (\hat{\mathbf{x}}_{k|k} - \mathbf{x}_k) (\hat{\mathbf{x}}_{k|k} - \mathbf{x}_k)^T \middle| R_k^* \right\} \geq [\mathbf{J}_k^*]^{-1}. \quad (29)$$

Daum [14] has shown (in the context of data association) that on average  $\mathbf{C}_k \geq \mathbf{C}_k^*$ . Combining this with (29), we have:

$$\mathbf{C}_k \geq \mathbf{C}_k^* \geq [\mathbf{J}_k^*]^{-1} \quad (30)$$

which supports our statement that the bound based on the assumption that the correct regime sequence is known, is too conservative.

Next we consider numerical examples that demonstrate the bound and its role in the error performance prediction and the assessment of algorithms for tracking manoeuvring targets.

### 4.2 Numerical examples

Consider now a target moving in two dimensions with  $s = 3$  dynamic models and no process noise.

**Model 1.** The constant velocity (CV) model, with state vector defined as  $\mathbf{x}_k = [x_k \dot{x}_k y_k \dot{y}_k]^T$  and function  $\mathbf{f}_{k-1}(\mathbf{x}_{k-1}, r_k = 1) = \mathbf{F}_{cv} \mathbf{x}_k$ , where  $\mathbf{F}_{cv}$  is the same as stated in (20).

**Model 2.** The coordinated turn (CT) model [1, Sec.11.7], with  $\mathbf{x}_k = [x_k \dot{x}_k y_k \dot{y}_k \Omega]^T$  and  $\mathbf{f}_{k-1}(\mathbf{x}_{k-1}, r_k = 2) = \mathbf{F}_{ct}\mathbf{x}_k$ , where  $\Omega$  is the turn rate and

$$\mathbf{F}_{ct} = \begin{bmatrix} 1 & \frac{\sin \Omega T}{\Omega} & 0 & \frac{\cos \Omega T - 1}{\Omega} & 0 \\ 0 & \cos \Omega T & 0 & -\sin \Omega T & 0 \\ 0 & \frac{1 - \cos \Omega T}{\Omega} & 1 & \frac{\sin \Omega T}{\Omega} & 0 \\ 0 & \sin \Omega T & 0 & \cos \Omega T & 0 \\ 0 & 0 & 0 & 0 & 1 \end{bmatrix}. \quad (31)$$

**Model 3.** The constant acceleration (CA) model, with  $\mathbf{x}_k = [x_k \dot{x}_k \ddot{x}_k y_k \dot{y}_k \ddot{y}_k]^T$  and  $\mathbf{f}_{k-1}(\mathbf{x}_{k-1}, r_k = 3) = \mathbf{F}_{ca}\mathbf{x}_k$ , where  $\mathbf{F}_{ca}$  is the same as stated in (21).

The regime variable sequence  $R_k^*$  is defined for  $k = 1 \dots 100$  scans with model transitions as follows:  $r_1^* \dots r_{25}^* = 1$ ,  $r_{26}^* \dots r_{32}^* = 2$ ,  $r_{33}^* \dots r_{69}^* = 1$ ,  $r_{70}^* \dots r_{85}^* = 3$ , and  $r_{86}^* \dots r_{100}^* = 1$ . The sampling interval is  $T = 3s$  and the initial target state vector is  $\mathbf{x}_0 = [10000m, -220m/s, 0m/s^2, 20000m, 0m/s, 0m/s^2]^T$ . The target trajectory is shown in Figure 5(a).

When the target is in the CT regime, the turn rate is  $\Omega = -8 \text{ deg/s}$ . When in the CA regime, the accelerations in  $x$  and  $y$  are  $-1g$  and  $1g$ , respectively. The target velocity and acceleration are shown in Figure 5(b).

The measurements  $\mathbf{z}_k$  of equation (3) consist of target position with  $\mathbf{h}_k(\mathbf{x}_k, r_k = 1) = \mathbf{H}_{cv}\mathbf{x}_k$ ,  $\mathbf{h}_k(\mathbf{x}_k, r_k = 2) = \mathbf{H}_{ct}\mathbf{x}_k$  and  $\mathbf{h}_k(\mathbf{x}_k, r_k = 3) = \mathbf{H}_{ca}\mathbf{x}_k$  where

$$\mathbf{H}_{cv} = \begin{bmatrix} 1 & 0 & 0 & 0 \\ 0 & 0 & 1 & 0 \end{bmatrix} \quad \mathbf{H}_{ct} = \begin{bmatrix} 1 & 0 & 0 & 0 & 0 \\ 0 & 0 & 1 & 0 & 0 \end{bmatrix} \quad (32)$$

$$\mathbf{H}_{ca} = \begin{bmatrix} 1 & 0 & 0 & 0 & 0 & 0 \\ 0 & 0 & 0 & 1 & 0 & 0 \end{bmatrix}$$

and

$$\mathbf{R} = \begin{bmatrix} \sigma_x^2 & 0 \\ 0 & \sigma_y^2 \end{bmatrix} \quad (33)$$

where  $\sigma_x = \sigma_y = 200m$ .

The  $\mathbf{P}_0$  matrix is the same as presented in (24) due to  $r_1^* = 1$  (CV case) with  $\sigma_{\dot{x}} = \sigma_{\dot{y}} = 150m/s$ . When there is a switch from CV model to CT model or CV model to CA model, the information matrix is augmented as described in (18). The standard deviations used in the augmentation are  $\sigma_{\Omega} = -4 \text{ deg/s}$  and  $\sigma_{\ddot{x}} = \sigma_{\ddot{y}} = 1.5g$ .

To compare the CRLB we performed a set of Monte Carlo simulations and estimated the RMS error of the VS-IMM filter. The results of 1000 Monte Carlo runs are shown in Figure 6. The dashed line in Figure 6(a) indicates the measurement accuracy in target position. The  $\sqrt{\text{CRLB}}$  is the lower bound. The RMS

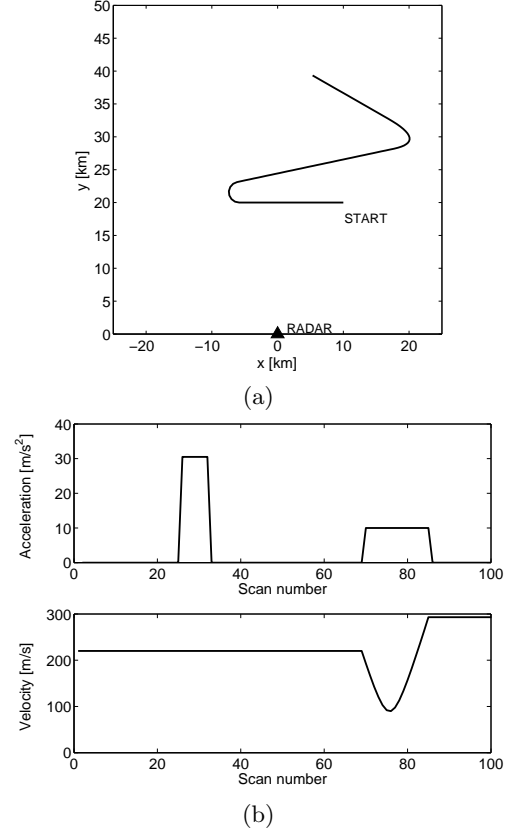
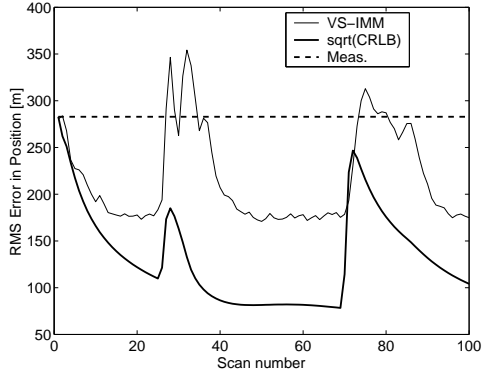


Figure 5: (a) Test trajectory consisting of CV-CT-CV-CA-CV segments; (b) Corresponding acceleration and velocity

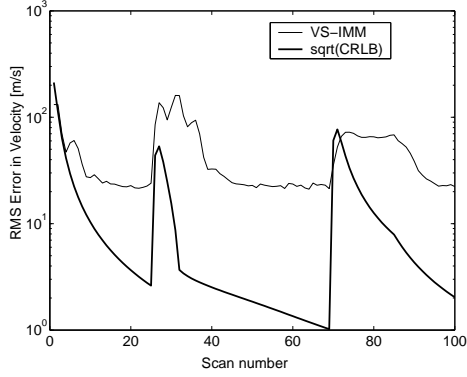
error in position of the VS-IMM follows the pattern of the  $\sqrt{\text{CRLB}}$  curve, exceeding the measurement bound at scan times when the target is manoeuvring. The RMS error in velocity behaves in a similar fashion, as shown in Figure 6(b).

**The influence of sampling time.** To test the influence of sampling time  $T$  on the CRLB, a target trajectory was generated using the above scenario for  $T_0 = 0.1s$ . From this data, trajectories were collated for each sample time interval  $T \geq T_0$ , to be compared. The CRLB curves in position and velocity for  $T$  values  $0.5s, 1s, 2s$  and  $4s$  are shown in Figure 7. The plots indicate that smaller values of  $T$  create a positive influence, decreasing the CRLB for both position and velocity.

**The influence of range rate measurements.** The influence of the addition of a range rate measurement on the CRLB was analysed using the scenario in section 4.2, with measurements  $\mathbf{z}_k$  of equation (3) consisting

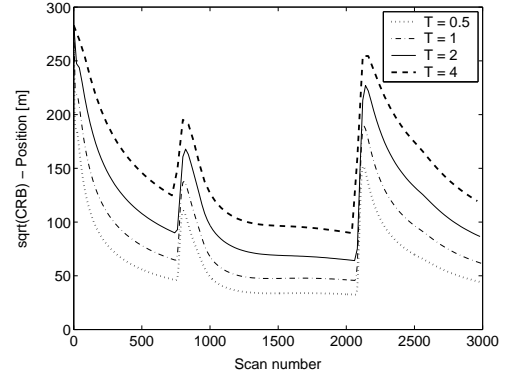


(a)

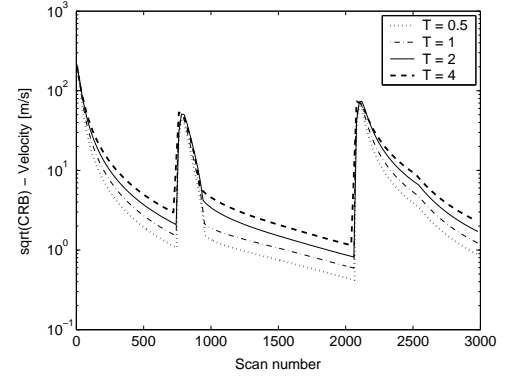


(b)

Figure 6: RMS Error in (a) position and (b) velocity for a deterministic trajectory vs  $\sqrt{\text{CRLB}}$ .



(a)



(b)

Figure 7:  $\sqrt{\text{CRLB}}$  in position (a) and velocity (b) for sample time values of 0.5s, 1s, 2s and 4s.

of target position and range rate with:

$$\mathbf{h}_k(\mathbf{x}_k) = \begin{bmatrix} x_k \\ y_k \\ \frac{x_k \dot{x}_k + y_k \dot{y}_k}{\sqrt{x_k^2 + y_k^2}} \end{bmatrix} \quad (34)$$

The measurements covariance is

$$\mathbf{R} = \begin{bmatrix} \sigma_x^2 & 0 & 0 \\ 0 & \sigma_y^2 & 0 \\ 0 & 0 & \sigma_{\dot{r}} \end{bmatrix} \quad (35)$$

where  $\sigma_x = \sigma_y = 200\text{m}$  with  $\sigma_{\dot{r}}$  as range rate standard deviation. The corresponding Jacobians for CV, CT and CA models are:

$$\mathbf{H}_{cv,k} = \begin{bmatrix} 1 & 0 & 0 & 0 \\ 0 & 0 & 1 & 0 \\ I_k \sin \theta_k & \cos \theta_k & -I_k \cos \theta_k & \sin \theta_k \end{bmatrix} \quad (36)$$

$$\mathbf{H}_{ct,k} = \begin{bmatrix} 1 & 0 & 0 & 0 & 0 \\ 0 & 0 & 1 & 0 & 0 \\ I_k \sin \theta_k & \cos \theta_k & -I_k \cos \theta_k & \sin \theta_k & 0 \end{bmatrix} \quad (37)$$

$$\mathbf{H}_{ca,k} = \begin{bmatrix} 1 & 0 & 0 & 0 & 0 & 0 \\ 0 & 0 & 0 & 1 & 0 & 0 \\ I_k \sin \theta_k & \cos \theta_k & 0 & -I_k \cos \theta_k & \sin \theta_k & 0 \end{bmatrix} \quad (38)$$

respectively, with

$$\theta_k = \arctan\left(\frac{y_k}{x_k}\right) \quad (39)$$

$$I_k = \frac{\dot{x}_k \sin \theta_k - \dot{y}_k \cos \theta_k}{\sqrt{x_k^2 + y_k^2}} \quad (40)$$

The CRLB curve was tested over various values of  $\sigma_{\dot{r}}$  to discover if the addition of a range rate measurement influenced the bound, when compared with the  $\sqrt{\text{CRLB}}$  in Figure 6. The position and velocity  $\sqrt{\text{CRLB}}$  curves for  $\sigma_{\dot{r}}$  values of 0.1m/s, 1m/s, and  $\infty$  are shown in Figure 8.

Figure 8 demonstrates that the inclusion of range rate has a positive effect on the CRLB. As  $\sigma_{\dot{r}}$  decreases in value the  $\sqrt{\text{CRLB}}$  decreases, with great improvement at scan times when the target is manoeuvring.

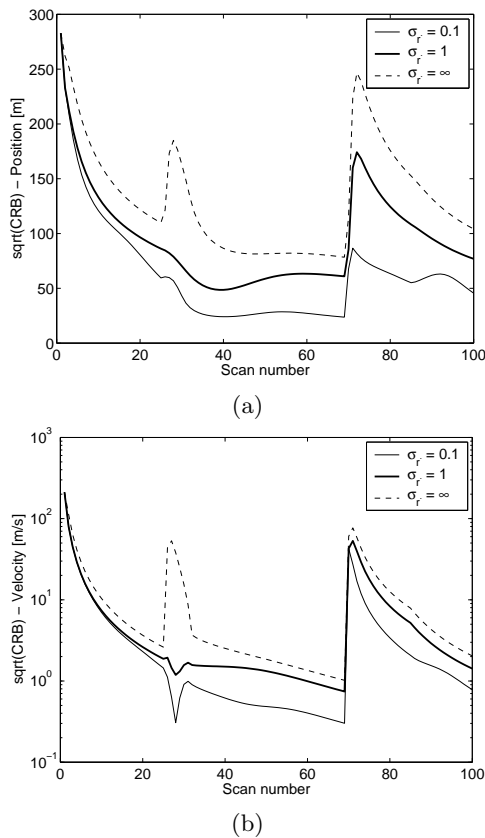


Figure 8:  $\sqrt{\text{CRLB}}$  in position (a) and velocity (b) for  $\sigma_r$  values of 0.1m/s, 1m/s and  $\infty$ .

## 5 Conclusions

The subject of Cramér-Rao type lower bounds for tracking a manoeuvring target has been investigated. Bounds for both random and deterministic trajectories have been considered. It has been demonstrated that for random manoeuvring targets a theoretical CRLB for an unbiased state estimator  $\hat{\mathbf{x}}_{k|k}$  can be computed. Using the probabilities of regime variable sequences and exploiting the structure of the TPM a conservative CRLB can be obtained, with limited computation required. The CRLB of a deterministic target trajectory was calculated, but was shown to be too conservative, due to the assumption that the correct regime sequence is known. Also demonstrated was that smaller sample times and the inclusion of range rate measurements decreases the CRLB.

## References

[1] Y. Bar-Shalom, X. R. Li, and T. Kirubarajan. *Estimation with Applications to Tracking and Navigation*. John Wiley & Sons, 2001.

[2] X. R. Li. Engineer's guide to variable-structure multiple-model estimation for tracking. In Y. Bar-Shalom and W. D. Blair, editors, *Multitarget-Multisensor Tracking: Applications and Advances*, volume III, chapter 10, pages 499–567. Artech House, 1993.

[3] A. H. Jazwinski. *Stochastic Processes and Filtering Theory*. Academic Press, 1970.

[4] F. Gustafsson. *Adaptive Filtering and Change Detection*. Wiley, 2000.

[5] J. H. Taylor. The Cramer-Rao estimation error lower bound computation for deterministic nonlinear systems. *IEEE Trans. Automatic Control*, 24(2):343–344, April 1979.

[6] T. H. Kerr. Status of CR-like lower bounds for nonlinear filtering. *IEEE Trans. Aerosp. Electr. Syst.*, 25(5):590–601, Sept. 1989.

[7] P. Tichavsky, C. H. Muravchik, and A. Nehorai. Posterior Cramér-Rao bounds for discrete-time nonlinear filtering. *IEEE Trans. Signal Processing*, 46(5):1386–1396, May 1998.

[8] A. Farina, B. Ristic, and L. Timmoneri. Cramer-Rao bound for nonlinear filtering with  $P_d < 1$  and its application to target tracking. *IEEE Trans. Signal Processing*, 50(8):1916–1924, August 2002.

[9] M. L. Hernandez, A. D. Marrs, N. G. Gordon, S. R. Maskell, and C. M. Reed. Cramér-Rao bounds for non-linear filtering with measurement origin uncertainty. In *Proc. 5th Int. Conf. Information Fusion*, volume 1, pages 18–25, Annapolis, MD, 2002.

[10] A. Farina and F. A. Studer. *Radar Data Processing (Vol. 1)*. John Wiley, 1985.

[11] W. D. Blair, G. A. Watson, T. Kirubarajan, and Y. Bar-Shalom. Benchmark for radar allocation and tracking in ECM. *IEEE Trans. Aerospace and Electronic Systems*, 34(4):1097–1113, Oct. 1998.

[12] X. Wang, S. Challa, and R. Evans. Variable structure IMM using minimal sub-model-set switching. In *Proc. SPIE: Signal Processing, Sensor Fusion and Target Recognition XII*, Orlando, FL, USA, April 2003.

[13] H. L. VanTrees. *Detection, Estimation and Modulation Theory (Part I)*. John Wiley & Sons, 1968.

[14] F. E. Daum. Bounds on performance for multiple target tracking. *IEEE Trans. Automatic Control*, 35(4):443–446, 1990.